

Promoted Catalysts for Hydrogenation of Bicyclic Aromatic Hydrocarbons Obtained in situ from Molybdenum and Tungsten Carbonyls

E. M. Zakharyan^{a, *}, M. I. Onishchenko^{a, **}, and A. L. Maksimov^{a, b}

^a*Topchiev Institute of Petrochemical Synthesis, Russian Academy of Sciences, Moscow, 119991 Russia*

^b*Faculty of Chemistry, Moscow State University, Moscow, 119991 Russia*

*e-mail: Zakharyan@ips.ac.ru,

**e-mail: onishchenko@ips.ac.ru

Received June 4, 2017

Abstract—Promoted Mo and W catalysts have been prepared in situ via thermal decomposition of precursors, oil-soluble salts $\text{Mo}(\text{CO})_6$, $\text{W}(\text{CO})_6$, $\text{CoC}_{16}\text{H}_{30}\text{O}_4$, and $\text{NiC}_{16}\text{H}_{30}\text{O}_4$. TiO_2 , Al_2O_3 , and $\text{ZrO}(\text{NO}_3)_2 \cdot 6\text{H}_2\text{O}$ have been used as the acidic additives. Also, Mo and W unsupported sulfide catalysts have been prepared in the presence of elemental sulfur as the sulfiding agent. The catalysts have been characterized by transmission electron microscopy and X-ray photoelectron spectroscopy. The activity of the catalysts prepared in situ has been evaluated in the hydrogenation reaction of bicyclic aromatic hydrocarbons by the example of model mixtures of 10% solutions of naphthalenes (unsubstituted naphthalene, 1- and 2-methylnaphthalenes, and 1,5- and 2,3-dimethylnaphthalenes) in *n*-hexadecane. The effect of the precursor/acidic oxide ratio on the activity of the formed catalyst has been found. Hydrogenation of bicyclic aromatic hydrocarbons has been conducted at a hydrogen pressure of 2 and 5 MPa and a temperature of 380 and 400°C for 2 h. Hydrogenation of the unsubstituted aromatic ring has been preferable due to the absence of steric hindrances. The degree of conversion of *n*-hexadecane under the reaction conditions has been 1.5–7.5% depending on the reaction temperature. It has been found that the activity of the sulfided catalyst in the conversion of 1- and 2-methylnaphthalenes is inferior to the activity of the unsulfided analogue, while partial replacement of TiO_2 by Al_2O_3 results in a decrease in the conversion of the substrates as opposed to the unsulfided catalysts, in which the use of nanocrystalline Al_2O_3 promotes an increase in the conversion.

Keywords: hydrogenation, hydrocracking, molybdenum hexacarbonyl, tungsten hexacarbonyl, molybdenum disulfide, nanotitania, nanoalumina, unsupported catalyst, bicyclic aromatic hydrocarbons, naphthalenes

DOI: 10.1134/S0965544118010164

INTRODUCTION

Processes of conversion of polyaromatic hydrocarbons (HCs) play a pivotal role in the hydroprocessing of petroleum fractions. Generally, a hydrogenation reaction precedes the processes of carbon–carbon bond opening and isomerization in the hydrocracking processes. Hydrogenation of polyaromatic and naphthene-aromatic compounds (hydrodearomatization) of middle-distillate fractions, in particular, in the case of highly aromatic fractions of secondary processes (gas oils of catalytic cracking and coking), provides the possibility for the preparation of kerosenes and diesel fuels which comply with the limits of the Technical Regulations. In industry, bimetallic sulfide catalysts on the basis of Group V metals (tungsten and molybdenum) supported onto aluminum silicates are generally used in these processes [1–3]. Unsupported catalysts [4], including catalysts dispersed in hydrocarbon

raw materials as well, can serve as an alternative for such a type of systems [5].

The use of unsupported catalysts in the processes of hydrocracking and hydrogenation of aromatic HCs is characterized by an advantage such as the simplicity of the preparation due to the absence of the need for conducting the stage of application of metals (active hydrogenating components) onto a support as opposed to supported catalysts (the *ex situ* method) [6, 7]. Such systems can be obtained already during the hydrogenation, hydrocracking, or desulfurization reaction by the *in situ* method [8–10]. As the compounds of metals, their salts are generally used, the reduction of which to highly dispersed nanocrystalline metal powders in these processes occurs via pyrolysis because these hydroprocesses proceed at quite high temperatures (up to 420–450°C) [11]. The advantages of pyrolysis are the low concentration of impurities in

the particles being obtained and their narrow size distribution.

Among unsupported catalysts for the hydroconversion reactions of petroleum fractions [12, 13], catalysts on the basis of molybdenum and tungsten sulfides promoted by nickel or cobalt are used most often [14]. The addition of these promoters leads to a substantial increase in the catalytic activity due to the formation of additional sulfide (nickel or cobalt sulfide) and mixed (nickel/cobalt–tungsten sulfide) phases [15, 16].

The use of acidic components such as titanium, aluminum, and zirconium oxides, as well as their combinations, promotes an increase in the activity of the catalysts in hydroprocesses [17]. Particular interest of researchers is generated by titanium oxide, for which three crystallographic structures are characteristic, namely, rutile, brookite, and anatase, the latter of which, existing in the metastable state, is the most active in photocatalysis [18]. Also, there is information that TiO_2 in the form of a mixture of anatase and rutile possesses higher activity when compared to anatase or rutile individually [19]. In addition to the photocatalytic reactions [20, 21], it is used as the support for systems in the hydrogenation [22] and oxidation [23] reactions and as the adsorbent of, e.g., water vapor [24]. The high catalytic activity of the systems on the basis of nanosized TiO_2 is possibly associated not only with the small size of particles (up to 100 nm) but also with the large specific surface area and character of the interaction of the corresponding sulfide with the surface of the oxide.

In connection therewith, it was of interest to form in situ catalytic systems on the basis of oil-soluble precursors of molybdenum and tungsten, as well as sources of promoting additives, nickel and cobalt ethylhexanoates. In addition, a combination of these dispersed Mo and W catalysts with the additions of nanosized oxides (e.g., TiO_2 and Al_2O_3) as well as their precursors (zirconium oxonitrate) was proposed. The activity of the systems obtained was studied in the hydrogenation reactions of aromatic HCs by the example of naphthalene, 1- and 2-methylnaphthalenes, and 2,3- and 1,5-dimethylnaphthalenes.

EXPERIMENTAL

The following oil-soluble compounds were used in the work: molybdenum hexacarbonyl $\text{Mo}(\text{CO})_6$ (99.99%, Aldrich), tungsten hexacarbonyl $\text{W}(\text{CO})_6$ (99.99%, Aldrich), nickel(II) 2-ethylhexanoate $\text{Ni}(\text{C}_7\text{H}_{15}\text{COO})_2$ (a 78% solution in 2-ethylhexanoic acid, Aldrich), and cobalt(II) 2-ethylhexanoate $\text{Co}(\text{C}_7\text{H}_{15}\text{COO})_2$ (a 78% solution in 2-ethylhexanoic acid, Aldrich). A nanopowder of titanium oxide TiO_2 (a mixture of rutile and anatase, a particle size <100 nm, 99.8%, Aldrich), a nanopowder of aluminum oxide Al_2O_3 (a particle size of 15 nm, 99.8%,

Aldrich), and zirconium oxonitrate $\text{ZrO}(\text{NO}_3)_2 \cdot 6\text{H}_2\text{O}$ (99%, Aldrich) were used as the acidic additive components. Elemental sulfur was used as the sulfiding agent for the preparation of the sulfide forms of the catalysts.

Analysis

The structure and morphology of the obtained samples of the catalysts were studied using high-resolution transmission electron microscopy (TEM) with a JEOL JEM 2100 electron microscope at an accelerating voltage of 200 kV.

During the statistical evaluation of the size characteristics of more than 300 particles of the active component in various TEM images for each catalyst, the distribution of sulfide particles by their length and number of layers in multilayer agglomerates was obtained. The average length of the sulfide particles \bar{L} was calculated by formula (1)

$$\bar{L} = \frac{\sum l_i}{n}, \quad (1)$$

where l_i is the length of the i th crystallite and n is the number of crystallites.

The average number of layers in the sulfide particles \bar{N} was calculated by formula (2)

$$\bar{N} = \frac{\sum n_i N_i}{n}, \quad (2)$$

where n_i is the number of particles with N_i layers [25].

The catalysts were studied by X-ray photoelectron spectroscopy (XPS) using a VersaProbeII X-ray photoelectron spectrometer (ULVAC-PHI). A monochromatic $\text{AlK}\alpha$ radiation (1486.6 eV) with a power of 25 W was used for the excitation of photoelectron emission. The diameter of the analyzed area was 100 μm . The panoramic spectra were recorded at a pass energy of the analyzer (E_{pass}) of 117.4 eV and an increment of 1.0 eV. The high-resolution (HR) spectra were recorded at E_{pass} of 11.75 eV and an increment of 0.1 eV. The HR spectra of $\text{Ti}2p$ were recorded at E_{pass} of 23.5 eV and an increment of 0.2 eV. The deconvolution of the spectra was performed via the nonlinear method of least squares using the Gauss–Lorentz function.

Catalyst Testing and Product Analysis Procedures

Model feedstocks were 10% solutions of substrates (the bicyclic aromatic HCs unsubstituted naphthalene, 1- and 2-methylnaphthalenes, and 1,5- and 2,3-dimethylnaphthalenes) in n -hexadecane. A weighed amount of a substrate, as well as a calculated amount of the precursor compounds, was introduced into an insert tube, while adding oxides or their precursors (in the case of zirconium oxide) where necessary. Then

the insert was placed into a 20-mL steel autoclave. The experiments were conducted at 380 and 400°C and a hydrogen pressure of 2 and 5 MPa under intense stirring. The molar ratios were as follows: substrate/Mo of 18.4 : 1 and 36.8 : 1, substrate/W of 18.4 : 1, substrate/Ti of 2.4 : 1, 4.9 : 1, 7.3 : 1, 9.7 : 1, and 12.5 : 1, substrate/Al of 4.9 : 1 and 9.7 : 1, substrate/Zr of 70.2 : 1, substrate/Co of 37.2 : 1, and substrate/Ni of 37.2 : 1. The catalysts were sulfided in situ in the hydrocarbon raw materials by adding elemental sulfur in the amount of 2.5 wt % relative to the weight of the raw materials (a solution of a substrate in *n*-hexadecane). The autoclave was heated to the temperature of the experiment at a rate of 10 deg/min. Upon the completion of the experiment, the autoclave was brought up to room temperature and the catalyst was separated from the conversion products via centrifugation. No formation of the gaseous products of the conversion of the raw materials was observed.

The obtained products of the experiments were analyzed on a Kristallyuks 4000 M chromatograph equipped with a flame ionization detector and an SPB-1 column (30 m × 0.25 mm) with a polydimethylsiloxane stationary liquid phase. The carrier gas was helium.

RESULTS AND DISCUSSION

Characterization of the Catalysts

The Mo–TiO₂ and sulfided MoS₂–TiO₂ (Ti/Mo = 3.8 : 1) catalysts formed during the hydrogenation reaction of a 10% solution of 2-methylnaphthalene in *n*-hexadecane at 380°C and 50 atm for 2 h and separated from the conversion products via centrifugation were characterized by XPS and TEM. The concentration and valence state of the elements on the surface of the catalysts was determined by XPS.

Molybdenum can exist on the surface of the Mo–TiO₂ catalyst in the oxide phase MoO_x (Mo⁶⁺ and Mo⁴⁺) [26, 27] and in the form of Mo₂C [28] and Mo⁰ [29]. The deconvolution of the Mo3d level showed that about 29% molybdenum was in the oxide phase MoO_x (Mo⁶⁺) (Table 1). Molybdenum was also detected in the form of initial hexacarbonyl and metallic molybdenum Mo⁰ being formed during the hydrogenation reaction of naphthalene in the atmosphere of H₂ on the surface of TiO₂ (227.6 eV, 4.2%). The spectrum presented peaks at 229.2 (29.8%) and 232.0 eV (37.5%) which, according to [29], correspond to the initial precursor Mo(CO)₆ (3d_{5/2}) and Mo(CO)₆ (3d_{3/2}) adsorbed on the surface of TiO₂.

The electron states Ti2p_{1/2} and Ti2p_{3/2} correspond to two peaks with the bond energy of 464.3 (32.1%) and 458.6 eV (67.9%), which confirms the presence of Ti⁴⁺ in the lattice of TiO₂ [27].

In the MoS₂–TiO₂ sulfided catalyst, molybdenum can exist on its surface both in the form of molybde-

num disulfide MoS₂ and in the oxide phase MoO_x, as well as in the intermediate state, in the form of molybdenum oxysulfide MoO_xS_y [30, 31]. The results of the deconvolution of the Mo3d level give the evidence of the fact that all the molybdenum is in the sulfide form, which suggests 100% sulfidation of the final material obtained (Table 1). No molybdenum in the form of oxide MoO_x and oxysulfide MoO_xS_y was detected (Table 1). The peak detected at 225.7 eV corresponds to sulfide sulfur S²⁻.

Like in the case of the Mo–TiO₂ catalyst, titanium is in the oxide form TiO₂ (*E*_b(Ti2p_{1/2}) = 464.1 eV and *E*_b(Ti2p_{3/2}) = 458.8 eV) [27]. It should also be noted that characteristic satellites were present in the spectrum of titanium [31].

Sulfur can be present on the surface of the catalyst in the form of both sulfur S²⁻ (MoS₂) and the S₂²⁻ phase (MoO_xS) [31, 33, 34]. According to the deconvolution, sulfur is present on the surface of the catalyst only in the form of sulfide S²⁻ (161.4 eV S2p_{3/2} and 162.6 eV S2p_{1/2}) (Table 1).

The analysis of the TEM images of the Mo–TiO₂ catalyst prepared in situ from the Mo(CO)₆ precursor and TiO₂ additive showed that agglomerates of TiO₂ and Mo particles were formed; the diameter of the former varied from 30 to 62 nm (Fig. 1). The lines highlighted in white correspond to the (101) plane of anatase TiO₂ [35].

The MoS₂–TiO₂ sulfided catalyst is characterized by a layered structure (Fig. 2) and consists of MoS₂ nanoplates, which is evidenced by the interplanar distance of 0.64–0.75 nm characteristic for the (002) basal plane of a molybdenum disulfide crystallite [36]. These particles are combined-into-agglomerates nanoplates [37] localized on the surface of TiO₂ particles with the (002) lattice of the hexagonal phase [35].

It was found on the basis of the statistical processing during the analysis of several micrographs of the MoS₂–TiO₂ sulfided catalyst that the average length of the particles of the active component of the catalyst was 4.5 nm, while the average number of layers in the multilayer agglomerate was four.

Catalytic Properties

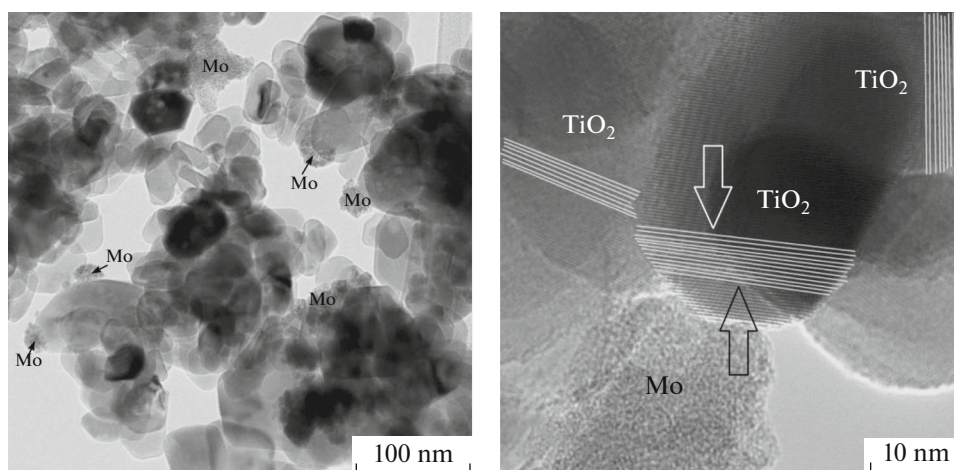
The dependence of the conversion of the substrate on the substrate/molybdenum and TiO₂/Mo(CO)₆ ratios in the raw materials is presented in Fig. 3 by the example of hydrogenation of 2-methylnaphthalene in the presence of the Mo–TiO₂ catalyst at 400°C and 2 MPa for 2 h. The highest conversion of the substrate is achieved at a TiO₂/Mo(CO)₆ ratio of 7.5 : 1 and a substrate/molybdenum ratio of 18.4 : 1 (44.6%) and 36.8 : 1 (43.9%). The main reaction products are 2- and 6-methyltetralines; no decalins are formed in the system; here, 6-methyltetraline is predominantly

Table 1. Data of XPS for the Mo3*d*, Ti2*p*, and S2*p* levels for the Mo–TiO₂ and MoS₂–TiO₂ catalysts

Catalyst	Element		Bond energy, eV weight fraction, %	State
Mo–TiO ₂ (Ti/Mo = 3.8 : 1)	Mo3 <i>d</i>	3 <i>d</i> _{5/2}	232.8 (22.5%)	MoO _x (Mo ⁶⁺)
		3 <i>d</i> _{3/2}	235.9 (6.0%)	
		3 <i>d</i> _{5/2}	229.2 (29.8%)	Mo(CO) ₆ (Mo ⁶⁺)
		3 <i>d</i> _{3/2}	232.0 (37.5%)	
	Ti2 <i>p</i>	3 <i>d</i> _{3/2}	227.6 (4.2)	Mo ⁰
		2 <i>p</i> _{3/2}	458.6 (67.9%)	TiO ₂ (Ti ⁴⁺)
Sulfided MoS ₂ –TiO ₂ , (Ti/Mo = 3.8 : 1, 2.5% S)	Mo3 <i>d</i>	2 <i>p</i> _{1/2}	464.3 (32.1%)	
		3 <i>d</i> _{5/2}	228.4 (57.3%)	MoS ₂
		3 <i>d</i> _{3/2}	231.6 (37.0%)	
		3 <i>d</i> _{5/2}	230.1 (0%)	MoO _x S _y
		3 <i>d</i> _{3/2}	233.2 (0%)	
		3 <i>d</i> _{5/2}	232.1 (0%)	MoO _x
	S2 <i>p</i>	3 <i>d</i> _{3/2}	235.2 (0%)	
		2 <i>p</i> _{3/2}	161.4 (73.1%)	S ^{2–}
		2 <i>p</i> _{1/2}	162.6 (26.9%)	
		2 <i>p</i> _{3/2}	163.5 (0%)	S ₂ ^{2–}
	Ti2 <i>p</i>	2 <i>p</i> _{1/2}	164.3 (0%)	
		2 <i>p</i> _{3/2}	458.8 (61.4%)	TiO ₂ (Ti ⁴⁺)
		2 <i>p</i> _{1/2}	464.1 (38.4%)	

formed (the 6-methyl-/2-methyl- ratio = 80 : 20). Increasing the pressure to 5 MPa promotes an increase in the conversion of the substrate by 15–20%, an insignificant decrease in the selectivity of the formation of 6-methyltetraline (the 6-methyl-/2-methyl-ratio = 70 : 30), as well as the formation of decalins (up to 14%).

Increasing the reaction time from 1 to 6 h leads to a small growth in the conversion of 2-methylnaphthalene from 37 to 44% (Fig. 4), which is due to the high reaction temperature and structure of the substrate. Also, the main reaction products are 2- and 6-methyltetralins. Even when conducting the reaction for 6 h, the concentration of decalins does not exceed 2%.

**Fig. 1.** Micrographs of the Mo–TiO₂ catalyst prepared in situ from the Mo(CO)₆ and TiO₂ precursors (Ti/Mo = 3.8 : 1).

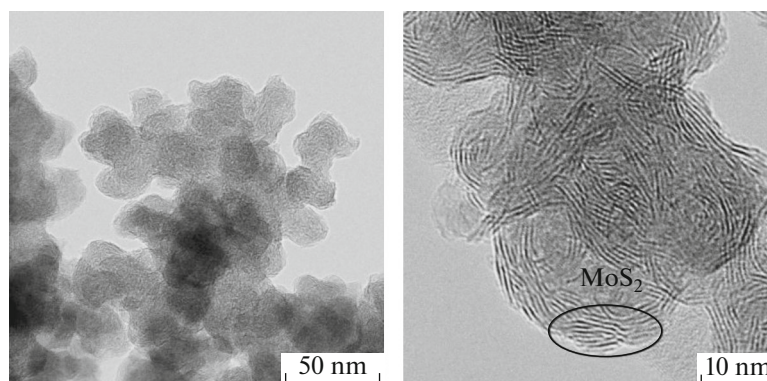


Fig. 2. Micrographs of the sulfided MoS_2 – TiO_2 catalyst prepared in situ from the $\text{Mo}(\text{CO})_6$ and TiO_2 precursors in the presence of elemental S ($\text{Ti}/\text{Mo} = 3.8 : 1$, 2.5% S).

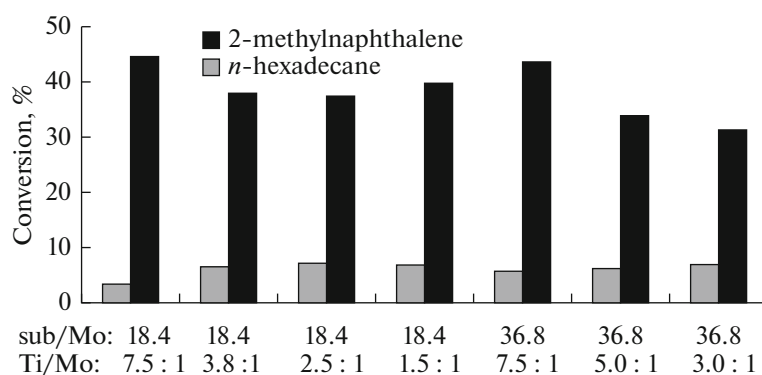


Fig. 3. The effect of the substrate/Mo and $\text{TiO}_2/\text{Mo}(\text{CO})_6$ ratios on the conversion of 2-methylnaphthalene (400°C, 2 MPa, 2 h).

The effect of the structural features of the substrate is demonstrated in Figs. 5a and 5b. In the case of the use of Mo – TiO_2 (substrate/Mo = 18.4 and $\text{Ti}/\text{Mo} = 3.8 : 1$) as the catalyst in hydrogenation of unsubstituted naphthalene, the maximum conversion is achieved at both 400 and 380°C, 69 and 99%, respectively. The presence of a methyl group in position 1 of naphthalene substantially decreases the yield of tetralins (to 39 and 41%), which is due to the steric hindrances during the approach and adsorption of a substrate molecule by the active sites on the surface of the catalyst. The presence of a substituent in position 2 of naphthalene no longer has the same effect on the decrease in the degree of conversion (by just 7%).

A substantial effect on hydrogenation of naphthalenes is also caused by the process temperature and pressure. Thus, for example, when 2,3-dimethylnaphthalene is hydrogenated at 400°C and 2 MPa, the yield of the products is 43%, while in the case of a decrease by just 20°C and an increase by 3 MPa, it already is 80%. 2,3- and 6,7-dimethyltetralines are formed as the products; the fraction of decalins at 400°C and 2 MPa is 6%, while at 380°C and 5 MPa, 3%; the predominant formation of the 6,7-dimethyl isomer (the selectivity of up to 80%), in which the unsubstituted

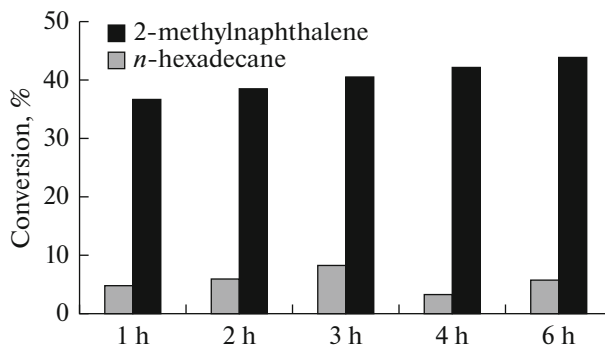


Fig. 4. The kinetics of the conversion of the model mixture of a 10% solution of 2-methylnaphthalene in n -hexadecane at 400°C and 2 MPa over the Mo/TiO_2 catalyst (substrate/Mo = 18.4, substrate/Ti = 4.9, and $\text{Ti}/\text{Mo} = 3.8 : 1$).

benzene ring is hydrogenated, is an interesting characteristic feature of the processes under these conditions. The small fraction of the second isomeric product being formed, 2,3-dimethyltetraline, is explained by the steric hindrances created by the methyl substituents in the benzene ring during the adsorption of the substrate on the surface of the catalyst.

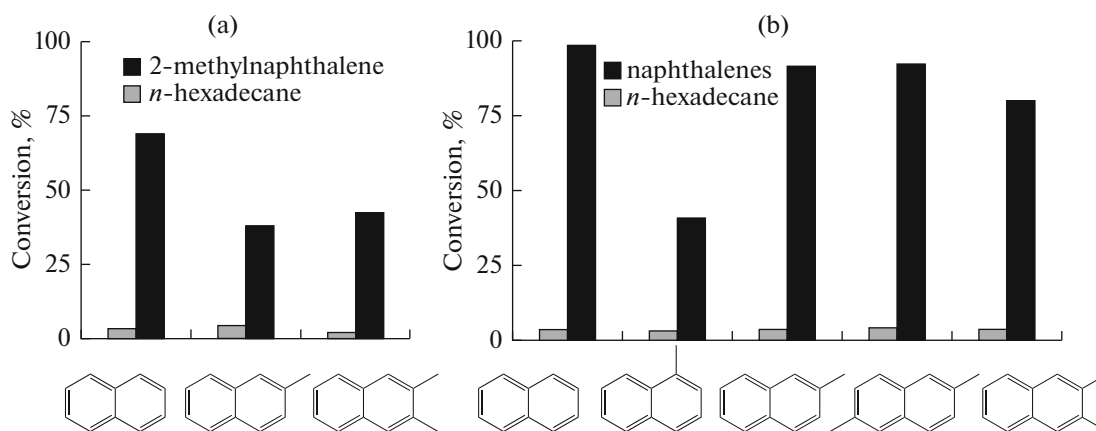


Fig. 5. The dependence of the conversion over the Mo-TiO₂ catalyst on the substrate type: (a) 400°C, 2 MPa, 2 h, substrate/Mo = 18.4, Ti/Mo = 3.8 : 1 and (b) 380°C, 5 MPa, 2 h, substrate/Mo = 18.4, Ti/Mo = 3.8 : 1.

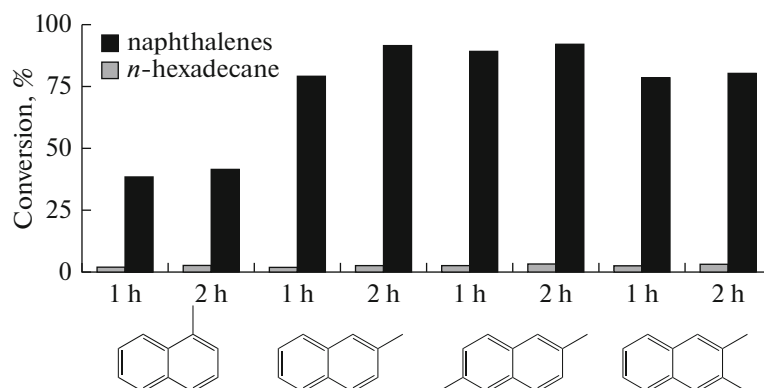


Fig. 6. The effect of the reaction time on the hydrocracking of 10% solutions of 1- and 2-methylnaphthalenes and 1,5- and 2,3-dimethylnaphthalenes in *n*-hexadecane over the Mo-TiO₂ catalyst at 380°C and 5 MPa (substrate/Mo = 18.4 and Ti/Mo = 3.8 : 1).

Figure 6 shows the effect of the reaction time (1 and 2 h) and presence of substituents in the substrate on the degree of its conversion. Like in the previous cases (Figs. 5a and 5b), the position of the substituent determines the activity of the catalyst and the yield of the product; the difference in the conversion of 1- and 2-methyl-substituted naphthalenes is 51% (the reaction time is 2 h). Such a great difference is determined by the fact that a competing process, isomerization of the substrate to 2-methylnaphthalene, occurs during hydrogenation of 1-methylnaphthalene [4]. The main products are 5- and 6-methyltetralines (the ratio is 75 : 25); the fraction of decalins in this process, in comparison with 2-methylnaphthalene, reaches 16%. Here, with the increase in the reaction time to 6 h, up to 61% decalins is formed (380°C, 5 MPa, Mo/TiO₂: substrate/Mo = 18.4, Ti/Mo = 3.8 : 1). The difference in the reaction times of 1 h has an unsubstantial effect on the yield of the process of hydrogenation of all the four substrates.

The partial and complete replacement of TiO₂ by acidic Al₂O₃ during the formation of the catalyst leads to a decrease in the conversion of 2-methylnaphthalene (380°C, 5 MPa, 2 h) from 91.8 to 71.3% (Table 2) and a decrease in the fraction of decalins, from 15.9 to 7.4%. The acidic OH groups on the surface of Al₂O₃ strongly interact with the OH groups of MoO₃, the main molybdenum phase of the Mo-Al₂O₃ catalyst, which leads to a change in the electron structure of the catalytic surface, thus increasing the acidity of the final catalyst, which adversely affects the adsorption of a substrate molecule. According to the published data, in the case of supported catalysts for hydrodesulfurization, CoMo/Al₂O₃ catalysts exhibit higher activity than CoMo/TiO₂ catalysts [38]. The addition of Co, Ni, and Zr promoters also promotes a decrease in the yield of the product, which acts conversely in the case of supported catalysts, namely, increases the catalytic activity of the catalysts [39]. Such a difference in the catalytic activity between unsupported and supported catalysts is possibly associated with the structural fea-

Table 2. The effect of additives on hydrogenation of 2-methylnaphthalene*

Catalyst	Substrate to metal, mol/mol	Metal 1/metal 2, mol/mol	Y_{dec} , %	$Y_{2\text{-mt}}$, %	$Y_{6\text{-mt}}$, %	$C_{2\text{-mn}}$, %	$C_{n\text{-C16}}$, %
Mo(CO) ₆ TiO ₂	Mo 18.4 Ti 4.9	Ti/Mo, 3.8 : 1	15.9	23.8	52.3	91.8	3.5
Mo(CO) ₆ TiO ₂ + Al ₂ O ₃	Mo 18.4 Ti 7.4 Al 7.4	Ti/Al/Mo, 1.9 : 1.9 : 1	8.9	23.2	58.9	86.9	2.4
Mo(CO) ₆ Al ₂ O ₃	Mo 18.4 Al 4.9	Al/Mo, 3.8 : 1	7.4	27.8	64.8	71.3	2.4
Mo(CO) ₆ + TiO ₂ ZrO(NO ₃) ₂ · 6H ₂ O	Mo 18.4 Zr 70.2 Ti 4.9	Zr/Ti/Mo 1 : 14.4 : 3.8	10.9	26.1	58.7	85.6	2.1
Mo(CO) ₆ + TiO ₂ + CoC ₁₆ H ₃₀ O ₄	Mo 18.4 Ti 4.9 Co 37.2	Ti/Mo/Co 7.6 : 2 : 1	12.7	23.9	49.3	72.3	3.1
Mo(CO) ₆ + TiO ₂ + NiC ₁₆ H ₃₀ O ₄	Mo 18.4 Ti 4.9 Ni 37.2	Ti/Mo/Ni 7.6 : 2 : 1	6.7	21.3	46	91.4	1.9

*The substrate is a 10% solution of 2-methylnaphthalene in *n*-hexadecane, 1.25 mmol. Reaction conditions: 2 h, 5 MPa H₂, and $T = 380^\circ\text{C}$. $C_{2\text{-mn}}$ is the conversion of 2-methylnaphthalene, %; $C_{n\text{-C16}}$ is the conversion of 2-methylnaphthalene, %; Y_{dec} is the yield of decalins, %; $Y_{2\text{-mt}}$ is the yield of 2-methyltetraline, %; and $Y_{6\text{-mt}}$ is the yield of 6-methyltetraline, %.

tures and properties of nanocrystalline oxides TiO₂ and Al₂O₃. In this case, the degree of conversion of *n*-hexadecane does not exceed 3.5%, which is due to the low reaction temperature.

Unlike the case of 2-methylnaphthalene, the partial replacement of TiO₂ by Al₂O₃ (the ratio of 1 : 1) in the processes of transformation of 1-methylnaphthalene and 1,5- and 2,3-dimethylnaphthalenes promotes an insignificant increase in the conversion of the substrate by 2–4% (Fig. 7) and a decrease in the degree of conversion of *n*-hexadecane to 1.2%.

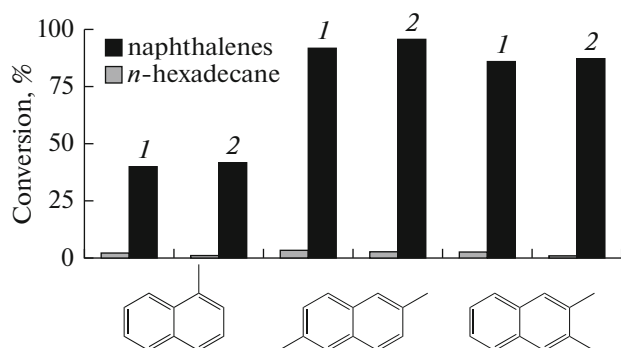


Fig. 7. The effect of the Al₂O₃ additive on the conversion of 10% solutions of 1-methylnaphthalene and 1,5- and 2,3-dimethylnaphthalenes in *n*-hexadecane over the Mo–TiO₂ catalyst: (1) substrate/Mo = 18.4 and Ti/Mo = 3.8 : 1 and (2) substrate/Mo = 18.4, Ti/Mo = Al/Mo = 1.9 : 1, and Ti/Al = 1 : 1 at 380°C and 5 MPa.

When conducting the hydrogenation reaction of 2-methylnaphthalene (400°C, 2 MPa, 2 h), the replacement of TiO₂ by Al₂O₃ also promotes an increase in the conversion in the case of the use of both Mo(CO)₆ and W(CO)₆ precursors (Fig. 8). The use of oil-soluble tungsten carbonyl leads to a significant decrease in the conversion, which is possibly explained by the change in its catalytic properties during the interaction with nanocrystalline oxides TiO₂ and Al₂O₃. A similar catalytic activity is also exhibited by sulfided Mo and W catalysts in hydrogenation of naphthalene [40].

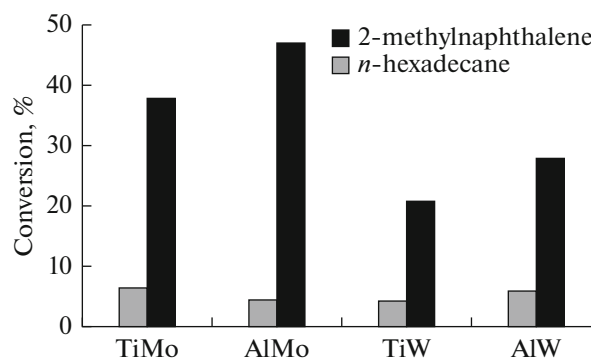


Fig. 8. The effect of precursors on the conversion of 2-methylnaphthalene (400°C, 2 MPa, 2 h). Reaction conditions: Mo–TiO₂, Mo–Al₂O₃, W–TiO₂, and W–Al₂O₃, substrate/Mo = substrate/W = 18.4, Ti/Mo = Al/Mo = Ti/W = Al/W = 3.8 : 1.

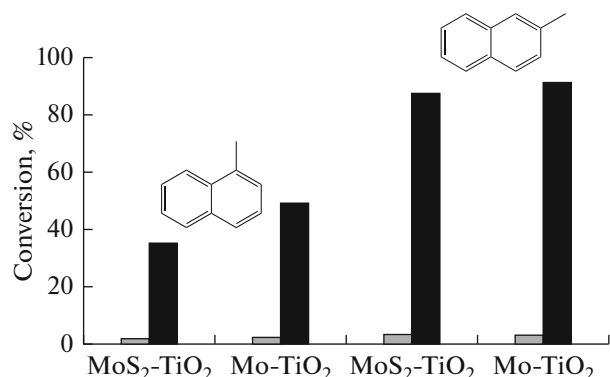


Fig. 9. The effect of the sulfidation of the catalyst on the conversion of 10% solutions of 1- and 2-methylnaphthalenes (Mo-TiO₂ and MoS₂-TiO₂ catalysts, substrate/Mo = 18.4 : 1, Ti/Mo = 3.8 : 1, 380°C, 5 MPa, 2 h).

The sulfided catalysts prepared in situ were also studied in the hydrogenation reactions of various naphthalenes. Molybdenum sulfide MoS₂ particles localized on the surface of TiO₂ nanoparticles served as the active catalytic sites in these catalysts (Fig. 2). As is seen from Fig. 9, the MoS₂-TiO₂ unsupported sulfided catalyst is characterized by lower activity, thus, 1- and 2-methylnaphthalenes are converted to a smaller extent in comparison with Mo-TiO₂ (380°C, 5 MPa, 2 h); here, the effect of the position of the substituent in the substrate is preserved. The yield of decalins did not exceed 10%.

The effect of the substrate/Mo ratio is presented in Fig. 10 by the example of the MoS₂-TiO₂ catalyst. The highest conversion was reached at the substrate/Mo ratio of 18.4 : 1 and the Ti/Mo ratio of 3.8 : 1 and 2.5 : 1 (400°C, 2 MPa, 2 h). The conversion declined substantially with the increase in the substrate/Mo ratio.

When passing from unsubstituted naphthalene to 2,3-dimethylnaphthalene (Fig. 11a), the conversion

sharply decreases, which is due to the effect of steric hindrances (MoS₂-TiO₂, substrate/Mo = 18.4 : 1, Ti/Mo = 3.8 : 1, 400°C, 2 MPa, 2 h). The conversion of *n*-hexadecane under these conditions does not exceed 4–7%.

In the case of a decrease in the temperature and an increase in the pressure (Fig. 11b), the conversion of naphthalene increases to 96%, the conversion of 2-methylnaphthalene, to 80%, and the conversion of 2,3-dimethylnaphthalene, to 90% (380°C, 5 MPa, 2 h), while the degree of conversion of *n*-hexadecane decreases to 2–3%. The effect of the position of the substituents is also seen from Fig. 11, namely, in the case of hydrogenation of 1-methylnaphthalene, during which the percent of isomerization of the substrate to 2-methylnaphthalene is significant.

Also, the effect of the nature of the additives (Table 3) and precursors (Fig. 12) was studied by the example of hydrogenation of 2-methylnaphthalene (MoS₂-TiO₂, 400°C, 2 MPa, 2 h). The use of the precursor of zirconium oxide, ZrO(NO₃)₂ · 6H₂O, (substrate/Zr = 70.2) promotes a decrease in the conversion of the substrate by 24%, while in the case of the addition of oil-soluble nickel ethylhexanoate NiC₁₆H₃₀O₄ (substrate/Ni = 37.2), the conversion increases to 53.3%, and the yield of decalins, to 8.1%.

In comparison with molybdenum hexacarbonyl Mo(CO)₆, the use of the W(CO)₆ precursor did not show high results (Fig. 12) (substrate/Mo = substrate/W = 18.4 : 1, Ti/Mo = Al/Mo = Ti/W = Al/W = 3.8 : 1).

The replacement of TiO₂ by more acidic Al₂O₃ also led to a decrease in the conversion of the substrate as opposed to the unsulfided catalysts, in which the use of nanocrystalline Al₂O₃ promoted an increase in the conversion (Fig. 8).

With the increase in the reaction time from 2 to 6 h, the conversion of 2-methylnaphthalene increases from 38 to 46.8%, and the conversion of *n*-hexadec-

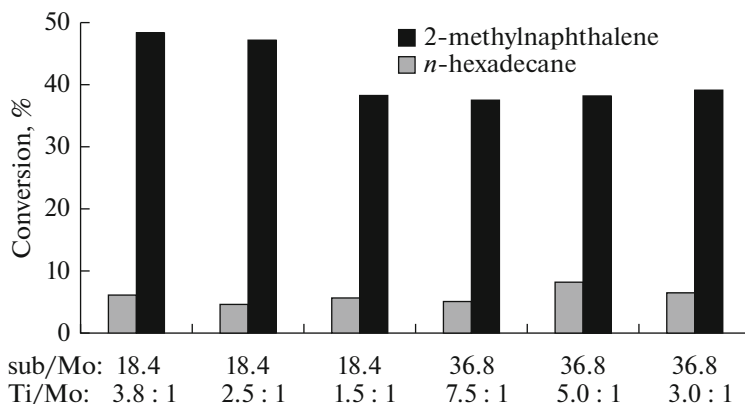


Fig. 10. The effect of sub/Mo and Ti/Mo ratios on the conversion of 2-methylnaphthalene (MoS₂-TiO₂, 400°C, 2 MPa, 2 h).

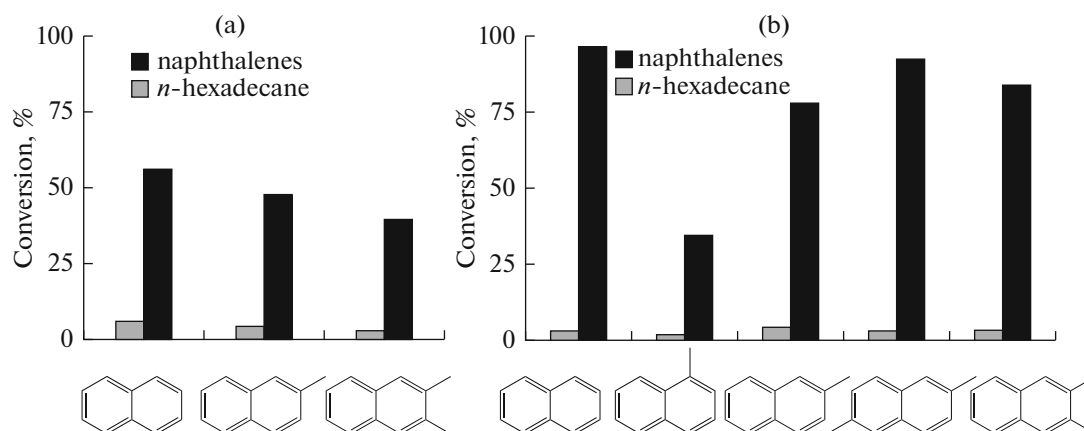


Fig. 11. The dependence of the conversion over the $\text{MoS}_2\text{--TiO}_2$ catalyst on the substrate type: (a) 400°C , 2 MPa, 2 h, substrate/Mo = 18.4 : 1, Ti/Mo = 3.8 : 1 and (b) 380°C , 5 MPa, 2 h, substrate/Mo = 18.4 : 1, Ti/Mo = 3.8 : 1.

ane, from 6.1 to 7.3% ($\text{MoS}_2\text{--TiO}_2$, substrate/Mo = 36.8, 400°C , 2 MPa, 2 h).

CONCLUSIONS

Unsupported Mo– TiO_2 and W– TiO_2 catalysts promoted by nickel and cobalt, as well as their sulfided analogues, have been obtained in the work by the in situ method. It has been found by X-ray photoelectron spectroscopy that, in the $\text{MoS}_2\text{--TiO}_2$ sulfided catalysts, all the molybdenum is in the composition of

sulfide MoS_2 , which suggests a 100% sulfidation of the metal. The formation of highly dispersed MoS_2 particles located on the surface of TiO_2 has been found by transmission electron microscopy. It has been shown that the catalysts exhibit high activity in the hydrogenation reactions of unsubstituted naphthalene, 1- and 2-methyl-naphthalenes, and 1,5- and 2,3-dimethylnaphthalenes and selectivity towards the formation of tetralins. The effect of aluminum and zirconium oxide additives has been studied. The effect of the substrate/precursor and precursor/acidic oxide ratios

Table 3. The effect of additives to the sulfided catalyst on hydrogenation of 2-methylnaphthalene*

Precursors	Substrate to metal, mol/mol	Metal 1/metal 2, mol/mol	Y_{dec} , %	$Y_{2\text{-mt}}$, %	$Y_{6\text{-mt}}$, %	$C_{2\text{-mn}}$, %	$C_{n\text{-C16}}$, %
$\text{Mo}(\text{CO})_6$ TiO_2	Mo 18.4 Ti 4.9	Ti/Mo, 3.8 : 1	4	14	29	48.3	6.2
$\text{Mo}(\text{CO})_6 + \text{TiO}_2$ + $\text{ZrO}(\text{NO}_3)_2 \cdot 6\text{H}_2\text{O}$	Mo 18.4 Ti 4.9 Zr 70.2	Zr/Ti/Mo, 1 : 14.4 : 3.8	3	12	31	34.1	5.9
$\text{Mo}(\text{CO})_6 + \text{ZrO}(\text{NO}_3)_2 \cdot 6\text{H}_2\text{O}$ + $\text{CoC}_{16}\text{H}_{30}\text{O}_4$	Mo 18.4 Zr 70.2 Co 37.2	Zr/Co/Mo, 1 : 2 : 4	5	12	29	45.4	6.4
$\text{Mo}(\text{CO})_6 + \text{ZrO}(\text{NO}_3)_2 \cdot 6\text{H}_2\text{O}$ + $\text{NiC}_{16}\text{H}_{30}\text{O}_4$	Mo 18.4 Zr 70.2 Ni 37.2	Zr/Ni/Mo, 1 : 2 : 4	2	7	15	24.6	8.5
$\text{Mo}(\text{CO})_6 + \text{TiO}_2$ + $\text{CoC}_{16}\text{H}_{30}\text{O}_4$	Mo 18.4 Ti 4.9 Co 37.2	Ti/Mo/Co, 7.6 : 2 : 1	3	7	19	28.4	6.5
$\text{Mo}(\text{CO})_6 + \text{TiO}_2$ + $\text{NiC}_{16}\text{H}_{30}\text{O}_4$	Mo 18.4 Ti 4.9 Ni 37.2	Ti/Mo/Ni, 7.6 : 2 : 1	8	14	32	53.3	2.9

*The substrate is a 10% solution of 2-methylnaphthalene in *n*-hexadecane, 1.25 mmol. Reaction conditions: 2 h, 2 MPa H_2 , $T = 400^\circ\text{C}$. $C_{2\text{-mn}}$ is the conversion of 2-methylnaphthalene, %; $C_{n\text{-C16}}$ is the conversion of 2-methylnaphthalene, %; Y_{dec} is the yield of decalins, %; $Y_{2\text{-mt}}$ is the yield of 2-methyltetraline, %; and $Y_{6\text{-mt}}$ is the yield of 6-methyltetraline, %.

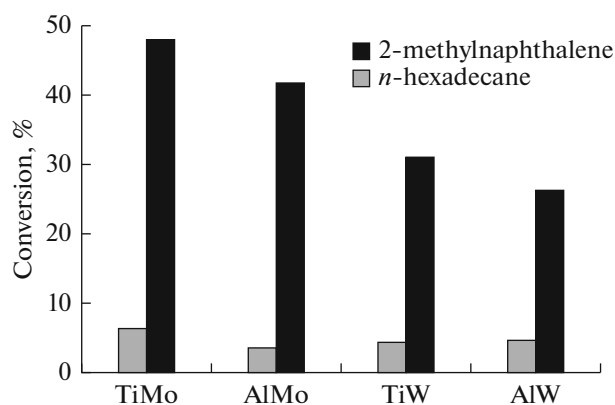


Fig. 12. The effect of the precursors on the conversion of 2-methylnaphthalene (400°C, 2 MPa, 2 h).

on the activity of the formed catalyst has been studied. The effect of the presence and position of methyl substituents in the substrates and reaction conditions including temperature and pressure on their conversion has been shown. It has been found that the activity of the sulfided catalyst in the conversion of 1-methyl- and 2-methylnaphthalenes is inferior to the unsulfided analogue. In addition, partial replacement of TiO_2 by Al_2O_3 leads to a decrease in the conversion of substrates as opposed to the unsulfided catalysts, in which the use of nanocrystalline Al_2O_3 promotes an increase in the conversion.

ACKNOWLEDGMENTS

The work was supported by the Russian Science Foundation, agreement no. 15-13-00123.

REFERENCES

1. R. Tian, B. Shen, F. Wang, et al., *Energy Fuels* **23**, 55 (2009).
2. M. J. Vissenberg, Y. van de Meer, E. J. M. Hensen, et al., *J. Catal.* **198**, 151 (2001).
3. E. J. M. Hensen, Y. van der Meer, J. A. R. van Veen, and J. W. Niemantsverdriet, *Appl. Catal., A* **322**, 16 (2007).
4. Y. Miki and Y. Sugimoto, *Fuel Process. Technol.* **43**, 137 (1995).
5. S. N. Khadzhiev, Kh. M. Kadiev, and M. Kh. Kadieva, *Pet. Chem.* **54**, 323 (2014).
6. P. Castillo-Villalon, J. Ramirez, R. Cuevas, et al., *Catal. Today* **259**, 140 (2015).
7. H. Zhang, Z. Wang, S. Li, et al., *Appl. Therm. Eng.* **111**, 811 (2017).
8. S. N. Khadzhiev, *Pet. Chem.* **56**, 465 (2016).
9. I. A. Sizova, A. B. Kulikov, M. I. Onishchenko, et al., *Pet. Chem.* **56**, 44 (2016).
10. Yu. V. Popov, V. M. Mokhov, D. N. Nebykov, and I. I. Budko, *Izv. Volgogradsk. Gos. Tekh. Univ.* **12**, 7 (2016).

11. H. Rezaei, X. Liu, S. J. Ardakani, et al., *Catal. Today* **150**, 244 (2010).
12. Y. G. Hur, D.-W. Lee, and K.-Y. Lee, *Fuel* **185**, 794 (2016).
13. U. S. Ozkan, L. Zhang, S. Ni, and E. Moctezuma, *Energy Fuels* **8**, 830 (1994).
14. D. Genuit, P. Afanasiev, and M. Vrinat, *J. Catal.* **235**, 302 (2005).
15. M. Sun, A. E. Nelson, and J. Adjaye, *J. Catal.* **226**, 41 (2004).
16. T. I. Koranyi, I. Manninger, Z. Paal, et al., *J. Catal.* **116**, 422 (1989).
17. S. Bagheri, N. M. Julkapli, and S. B. Abd Hamid, *Sci. World J.* **2014**, 1 (2014).
18. G. Li, L. Li, J. Boerio-Goates, and B. F. Woodfield, *J. Am. Chem. Soc.* **127**, 8659 (2005).
19. M. Francisco and V. Vastelaro, *Chem. Mater.* **14**, 2514 (2002).
20. I. Jang, J.-H. Park, K. Song, et al., *Mater. Chem. Phys.* **147**, 691 (2014).
21. D. M. Metzler, M. Li, A. Erdem, and C. P. Huang, *Chem. Eng. J.* **170**, 538 (2011).
22. J. Panpranot, K. Kontapakdee, and P. Praserttham, *Appl. Catal., A* **314**, 128 (2006).
23. A. Yoshida, Y. Takahashi, T. Ikeda, et al., *Catal. Today* **164**, 332 (2011).
24. A. N. Okte, D. Karamanis, and D. Tuncel, *Catal. Today* **230**, 205 (2014).
25. B. S. Zhang, Y. J. Yi, W. Zhang, et al., *Mater. Charact.* **62**, 684 (2011).
26. O. Aviles-Garcia, J. Espino-Valencia, R. Romero, et al., *Fuels* **198**, 31 (2017).
27. X. Cheng, X. Yu, and Z. Xing, *J. Colloid Interface Sci.* **372**, 1 (2012).
28. Y. Zhu, S. Wang, Y. Zhong, et al., *J. Power Sources* **307**, 552 (2016).
29. Zh. Jiang, W. Huang, Zh. Zhang, et al., *Surf. Sci.* **601**, 844 (2007).
30. T. K. T. Ninh, L. Massin, D. Laurenti, and M. Vrinat, *Appl. Catal., A* **407**, 29 (2011).
31. P. Li, Y. Chen, C. Zhang, et al., *Appl. Catal., A* **533**, 99 (2017).
32. M. Oku, H. Matsuta, K. Wagatsuma, et al., *J. Electron Spectrosc. Relat. Phenom.* **105**, 211 (1999).
33. A. Santoni, F. Rondino, C. Maleba, M. Valentini, A. Mittiga, *Appl. Surf. Sci.* **392**, 795 (2017).
34. M. A. Baker, R. Gilmore, C. Lenardi, and W. Gissler, *Appl. Surf. Sci.* **150**, 255 (1999).
35. X. Zhang, Ch. Shao, X. Li, et al., *J. Alloys Compd.* **686**, 137 (2016).
36. B. Yoosuk, J. H. Kim, C. Song, et al., *Catal. Today* **130**, 14 (2008).
37. L. Zhang, X. Long, D. Li, and X. Gao, *Catal. Commun.* **12**, 927 (2011).
38. H. K. Kim, Ch.-Wh. Lee, M. Kim, et al., *Int. J. Hydrogen Energy* **41**, 18846 (2016).
39. Y. Wu, G. Hu, Y. Xie, et al., *Solid State Sci.* **13**, 2096 (2011).
40. H. Liu, Ch. Liu, Ch. Yin, et al., *Catal. Today* **276**, 46 (2016).

Translated by E. Boltukhina